HHS Public Access

Author manuscript

Stroke. Author manuscript; available in PMC 2021 November 01.

Published in final edited form as:

Stroke. 2020 November ; 51(11): 3320–3331. doi:10.1161/STROKEAHA.120.029951.

Inhibition of EZH2 attenuates neuroinflammation via H3k27me3/SOCS3/TRAF6/NF-κB in a rat model of subarachnoid hemorrhage

Yujie Luo, M.D[1,#], **Yuanjian Fang, M.D**[1,#], **Ruiqing Kang, M.D**[2], **Cameron Lenahan, B.S**[2,3], **Marcin Gamdzyk, Ph.D**[2], **Zeyu Zhang, M.D**[1], **Takeshi Okada, M.D**[2], **Jiping Tang, M.D, Ph.D**[2], **Sheng Chen, M.D**[1,*], **John H Zhang, M.D, Ph.D**[2,*]

[1]Department of Neurosurgery, The Second Affiliated Hospital, School of Medicine, Zhejiang University, Hangzhou, Zhejiang Province, China

[2]Department of Physiology and Pharmacology, School of Medicine, Loma Linda University, Loma Linda, CA, USA

[3]Burrell College of Osteopathic Medicine, Las Cruces, NM, USA

Abstract

Background and Purpose: Neuroinflammation has been proven to play an important role in the pathogenesis of early brain injury (EBI) after subarachnoid hemorrhage (SAH). Enhancer of zeste homolog 2 (EZH2)-mediated trimethylation of histone 3 lysine 27 (H3K27Me3) has been recognized to play a critical role in multiple inflammatory diseases. However, there is still a lack of evidence to address the effect of EZH2 on the immune response of SAH. Therefore, the aim of this study was to determine the role of EZH2 in SAH-induced neuroinflammation and explore the effect of EZH2 inhibition with its specific inhibitor EPZ6438.

Methods: The endovascular perforation method was performed on rats to induce subarachnoid hemorrhage. EPZ6438, a specific EZH2 inhibitor, was administered intraperitoneally at 1h after SAH. Suppressor of cytokine signaling 3 (SOCS3) siRNA and H3K27me3 CRISPR were administered intracerebroventricularly at 48h before SAH to explore potential mechanisms. The SAH grade, short-term and long-term neurobehavioral tests, immunofluorescence staining, and western blots were performed after SAH.

Results: The expression of EZH2 and H3K27me3 peaked at 24h after SAH. In addition, inhibition of EZH2 with EPZ6438 significantly improved neurological deficits both in short-term and long-term outcome studies. Moreover, EPZ6438 treatment significantly decreased the levels of

[*]**Corresponding authors:** Sheng Chen, MD, Department of Neurosurgery, The Second Affiliated Hospital, School of Medicine, Zhejiang University, Hangzhou, Zhejiang Province, China, saintchan@zju.edu.cn. John H. Zhang, MD&PhD, Department of Physiology and Pharmacology, School of Medicine, Loma Linda University, 11041 Campus Street, Loma Linda, CA 92354, USA, johnzhang3910@yahoo.com.

[#]Yujie Luo and Yuanjian Fang contributed equally to this work.

Disclosures

None.

Supplemental Materials

Online Table I animal number.

Online Figures I SAH grade.

EZH2, H3K27Me3, pathway-related proteins tumor necrosis factor (TNF) receptor family 6 (TRAF6), nuclear factor-κB (NF-κB) p65, pro-inflammatory cytokines TNF-α, interleukin (IL)-6, IL-1β, but increased the expression levels of SOCS3 and anti-inflammatory cytokine IL-10. Furthermore, administration of SOCS3 siRNA and H3k27me3-activating CRISPR partly abolished the neuroprotective effect of EPZ6438, which indicated that the neuroprotective effect of EPZ6438 acted, at least partly, through activation of SOCS3.

Conclusions: In summary, the inhibition of EZH2 by EPZ6438 attenuated neuroinflammation via H3K27me3/SOCS3/TRAF6/NF-κB signaling pathway after SAH in rats. By targeting EZH2, this study may provide an innovative method to ameliorate EBI after SAH.

Graphical Abstract

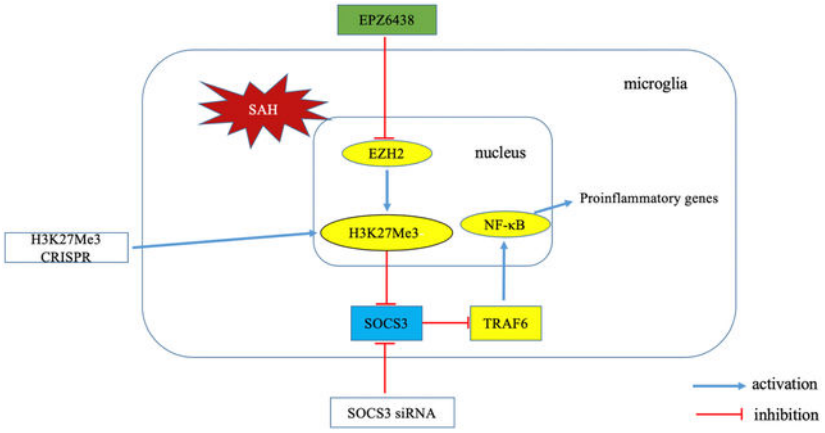

Keywords

subarachnoid hemorrhage; inflammation; EZH2; H3K27me3; neuroprotection

Introduction

Subarachnoid hemorrhage (SAH) is a type of cerebrovascular disease with high mortality and morbidity.[1] According to recent studies, early brain injury (EBI) may be the underlying cause of poor outcomes in patients with SAH. Among all possible mechanisms of EBI, neuroinflammation is now considered the main contributor of EBI.[2, 3] However, there is still a lack of effective pharmaceutical treatment for EBI. Therefore, the anti-inflammation treatment may be practical.

Enhancer of zeste homolog 2 (EZH2) is an essential component of polycomb repressive complex 2. It is also a histone methyltransferase, which catalyzes the repressive chromatin modification histone H3 lysine 27 trimethylation, eventually resulting in gene silencing.[4] There is emerging evidence showing the important role of EZH2 in inflammatory diseases, such as autoimmune inflammation, prostatitis, colitis, etc.[5, 6] Moreover, EZH2 regulated the immune responses in the central nervous system.[7] Inhibition of EZH2 attenuated neuroinflammation in neuropathic pain and provided neuroprotective effects in ischemic stroke.[8] EPZ6438, a potent and selective EZH2 inhibitor, is a promising treatment for non-Hodgkin Lymphoma because of its superior potency and oral bioavailability.[9, 10] EPZ6438

depleted EZH2 and downregulated the expression of trimethylation of histone 3 lysine 27 (H3K27Me3). Administration of EPZ6438 reduced microglial activation in a lipopolysaccharide- treated primary microglial cell vitro study.[7] In addition, suppressor of cytokine signaling 3 (SOCS3) is known as an intracellular negative regulator of inflammation.[11] EZH2-mediated H3K27me3 directly targets SOCS3 for its transcriptional inhibition. SOCS3 promoted Lys48-linked ubiquitination and degradation of tumor necrosis factor (TNF) receptor family 6 (TRAF6). SOCS3 mediated the degradation of TRAF6, which subsequently leads to the inhibition of nuclear factor-κB (NF-κB) activation.[12]

In the present study, we hypothesized that EPZ6438, as an inhibitor of EZH2, can attenuate neuroinflammation by reducing the expression of H3K27me3, and may be a potential therapeutic agent for SAH. These neuroprotective effects may be mediated through the SOCS3/TRAF6/NF-κB signaling pathway.

Methods

The original data of this current study can be obtained from the corresponding author on request. All animals were randomized to the control, and experimental groups and neurobehavioral testing, as well as quantitative data collection, was conducted in a blinded fashion (animals and sample tubes were marked by numbers, without any identifiers of group allocation).

Animals

Adult male Sprague-Dawley rats (10-week-old, 300–320g) were housed in a humidity controlled and constant temperature (25°C) room, with a 12-h light/dark cycle and free access to food and water. All experimental protocols were approved by the Institutional Animal Care and Use Committee of Loma Linda University and in accordance with the National Institutes of Health (NIH) guide for the care and use of laboratory animals.

SAH model

Endovascular perforation SAH model was induced in rats as previously described.[13] Briefly, the rats were anesthetized using 5% isoflurane. During surgery, the rats were ventilated with 3% isoflurane. After carefully exposing the left carotid artery, a 4–0 sharpened monofilament nylon suture was inserted into the external carotid artery. After feeling resistance at the bifurcation of the anterior and middle cerebral arteries, the monofilament nylon suture was advanced another 3mm to further puncture the vessel. After vessel perforation, the nylon suture was immediately withdrawn. The sham-operated animals underwent the same surgical procedure, but without vessel perforation. After removal of the suture, the incision was closed. The rats were housed individually in heated cages until they recovered from anesthesia.

Drug administration

EPZ6438 (TargetMol, USA) was dissolved in 10% DMSO and administered via intraperitoneal injection (*i.p*). Three different dosages of EPZ6438 (1mg/kg, 3mg/kg, 9mg/kg) were given to rats at 1h after SAH.[7] SOCS3 siRNA (Ambion, USA) was

administrated intracerebroventricularly. The same volume of 10% DMSO was given via *i.p* as the vehicle.

Intracerebroventricular injection

Intracerebroventricular injection (*i.c.v*) method was performed as previously reported.[14] Briefly, the rats were placed in a stereotaxic apparatus under 3% isoflurane anesthesia. A burr hole was drilled into the skull at the following coordinates relative to the bregma:1.5mm lateral, 0.9mm posterior, and the 10-μL Hamilton syringe was inserted into the burr hole at a depth of 3.3mm. SOCS3 siRNA (Ambion, USA) and control siRNA were infused into the right ventricle at a rate of 1 μL/min with a pump. H3K27me3 CRISPR (Santa Cruz Biotechnology, Dallas, TX, USA) was used to increase H3K27me3 gene expression. A total of 5ug per pup of H3K27me3 CRISPR or scrambled CRISPR (Santa Cruz Biotechnology, Dallas, TX, USA) was injected into the ipsilateral ventricle at 48h before SAH.

Experimental design

Experimental 1: time course and cellular localization of EZH2 and H3K27Me3 —In this part, 40 rats were randomly divided into sham, SAH (3h, 6h, 12h, 24h, 72h) groups. EZH2 and H3K27Me3 expression levels were detected by Western blot at every single time point (n=6 for each group). Immunofluorescence staining was used to show the colocalization of EZH2 and H3K27Me3 with microglia, astrocytes, and neurons in sham and SAH (n=2 for each group).

Experiment 2: short-term outcome study—To study the neuroprotective effect of EPZ6438, a total of 30 rats were randomly assigned into 5 groups with n=6 per group: sham, SAH + vehicle, SAH + EPZ6438 (1mg/kg), SAH + EPZ6438 (3mg/kg), SAH + EPZ6438 (9mg/kg). EPZ6438 was administered at 1h after SAH via *i.p*. Neurological scores and brain water content were measured at 24h after SAH.

To explore the efficacy of EPZ6438 on neuroinflammation, microglia activation and neutrophil infiltration were detected at 24h after SAH. An additional 9 rats were randomly divided into 3 groups with n=3 per group: sham, SAH + vehicle, SAH + EPZ6438 (3mg/kg).

Experiment 3: long-term outcome study—To explore the effects of EPZ6438 on long-term neurobehavioral function, a total of 30 rats were randomly assigned into 3 groups with n=10 per group: sham, SAH + vehicle, SAH + EPZ6438 (3mg/kg). To evaluate the sensorimotor coordination and balance ability of rats, the Rotarod test was performed at day 7, day 14, and day 21 after SAH. In addition, the Morris water maze was used to assess the spatial learning and memory of the rats, and it was performed on days 21–25 after SAH.

Experiment 4: mechanism study—Experiment 4 was divided into two parts. The first part was to explore the underlying mechanism of EPZ6438-mediated anti-neuroinflammation effects after SAH, SOCS3 siRNA was administered via *i.c.v* 48h before SAH. Thirty rats were randomly divided into 5 groups with n=6 per group: sham, SAH + vehicle, SAH + EPZ6438, SAH + EPZ6438 + SOCS3 si RNA, SAH + EPZ6438 + scr siRNA. Western blot was detected at 24h after SAH.

The second part was to assess the role of H3k27me3 on the anti-neuroinflammatory effects of EPZ6438, H3k27me3 activating CRISPR was administered by *i.c.v* 48h before SAH. An additional 12 rats were randomly divided into SAH+EPZ6438+H3k27me3 CRISPR and SAH+EPZ6438+scr CRISPR group (n=6 in each group) and then compared with sham, SAH + vehicle, SAH + EPZ6438 (shared with the first part). Western blot was detected at 24h after SAH.

SAH grade

SAH Grade was used to evaluate the severity of SAH as previously described.[15] Briefly, the basal cistern was divided into six sections, each section was given a grade of 0–3 according to the following criteria: 0 = no SAH; 1 = minimal SAH; 2 = SAH with recognizable vessels; 3 = SAH without recognizable vessels. The total scores ranged from 0 to 18, and the rats with scores < 8 were excluded from this study. SAH grade was evaluated in a blinded manner.

Brain water content

A wet-dry method was used to measure the brain water content as previously reported.[16] Briefly, the brains were divided into four parts: left hemisphere, right hemisphere, brain stem, and cerebellum. After harvesting the brains, each part was weighed immediately as the wet weight, and then weighed again after 72h at 100°C as the dry weight. Brain water content was calculated as (wet weight – dry weight)/wet weight × 100%.

Modified Garcia score and Beam balance test

Modified Garcia score and Beam balance test were performed in a blinded manner to assess the short-term neurological function as previously reported.[17] Briefly, the modified Garcia score is composed of six tests as follows: spontaneous activity, spontaneous movement of the four limbs, body proprioception, whisker proprioception, forepaw outstretching, and climbing. The total score was calculated as the sum of six tests with a cumulative score ranging from 3 to 18, with higher scores indicating better neurological function. Beam balance test is used to assess the rats' ability to walk on the wooden beam for 1 minute. The evaluation was as follows: 0 = not walk and fall; 1 = not walk but remains on beam; 2 = walk but fall; 3 = walk < 20 cm; 4 = walk beyond 20cm.

Rotarod test and Water Maze test

The rotarod test was performed on days 7, 14, and 21 to assess the sensorimotor coordination ability of animals by a blinded investigator as previously described.[18] Briefly, the rotarod speed started from 5rpm and 10rpm, with a 2rpm increase in speed every 5s. The duration of rats on the rotarod machine was recorded. The Morris water maze was performed at day 21–25 after SAH as previously described. On the last day, A 60s probe trial was performed on the rats' ability to find the platform, which had already been removed. Escape latency, probe quadrant duration, and swimming velocity were recorded by the tracking system.

Western blot analysis

Western blot was performed as previously reported.[19] Briefly, the rats were sacrificed at 3h, 6h, 12h, 24h, and 72h after SAH. Rats were anesthetized and perfused with 0.1M PBS, and the left hemispheres were immediately harvested. Samples were mixed with RIPA, after centrifuged at 14000g for 20min (4°C), the supernatants were collected. A protein assay kit was used for measuring the protein concentration of the samples. Equal amounts of proteins (40μg) were loaded onto the SDS-PAGE gel and transferred onto polyvinylidene fluoride membranes. Membranes were incubated with primary antibodies against EZH2 (1;1000, ab191080, Abcam, USA), H3K27Me3 (1:1000,ab6002, Abcam, USA), H3 (1:1000, ab1791, Abcam, USA), SOCS3(1:1000, ab14939, Abcam, USA), TRAF6 (1:1000, ab227560, Abcam, USA), NF-κB(1:1000, ab16502, Abcam, USA), IL-1β (1:1000, ab9722, Abcam, USA), IL-6 (1:1000, ab6672, Abcam, USA), TNF-α (1:1000, ab1793, Abcam, USA), and IL-10 (1:1000, ab33471, Abcam, USA) overnight at 4°C. On the following day, secondary antibodies were incubated at room temperature for 2h. The bands were visualized by ECL reagents. The proteins band densities were analyzed with Image J software.

Immunofluorescence

The rats were anesthetized with isoflurane and transcardially perfused with 0.1M PBS and followed with 10% formalin. The brains were immersed in 10% formalin for 48h at 4°C, and then dehydrated in 30% glucose for 72h. Brain samples were cut into 10-μm-thick coronal sections using a cryostat. Brain slices were rinsed and blocked with 5% donkey serum for 1h at room temperature. Slices were incubated with primary antibodies against EZH2 (1:200, ab191080, Abcam, USA), H3K27Me3 (1:200,ab6002, Abcam, USA), Iba-1 (1:200, ab5076, Abcam, USA), NeuN (1:200, ab103224, Abcam, USA), GFAP (1:200, ab53554, Abcam, USA), MPO (1:200, ab208670, Abcam, USA), CD16 (1:200, ab211151, Abcam, USA), CD206 (1:200, sc-70585, Santa Cruz, USA) overnight at 4°C. On the following day, the slices were incubated with fluorophore-conjugated secondary antibodies for 2h at room temperature. After adding DAPI, the brain slices were visualized under a fluorescence microscope.

Statistical analysis

All data were expressed as mean ± SD, statistical analyses were performed with Graph Pad Prism 6.0. One-way ANOVA, followed by Tukey's post-hoc test, was used to compare multiple groups; Two-way ANOVA, followed by Tukey's post-hoc test was used to compare the changes according to the different levels of multiple categorical variables (Brain water content, long-term neurological function). Statistical significance was defined as $P<0.05$.

Results

Mortality and SAH grade

A total number of 175 male rats were used in this study, and 5 rats were excluded for mild SAH grade. The total mortality of SAH rats was 13.9% (19/137), no rat died in sham group. (Supplementary Table I) There was no significant difference of SAH grade among all SAH

groups. (Supplementary Figure I) Blood clots were mainly distributed around the Circle of Willis in the SAH rats, but no blood clots were observed in sham rats.

Temporal patterns and cellular colocalization of EZH2 and H3K27Me3

Western blot was used to detect the protein levels of EZH2 and H3K27Me3 in sham, 3h ,6h, 12h, 24h, and 72h after SAH. Results showed that the EZH2 and H3K27Me3 expressions started to increase at 3h, peaked at 24h, and was down-regulated at 72h after SAH. (Figure1 A) Double immunofluorescence staining was performed to show the localization of EZH2 and H3K27Me3 with microglia, neurons, and astrocytes. EZH2 and H3K27Me3 were expressed in all three types of cells. (Figure 1B, C)

EPZ6438 treatment improved short-term neurobehavioral functions and reduced brain edema after SAH

Modified Garcia score and Beam Balance test were performed to assess the neurological functions at 24h after SAH. After SAH, the modified Garcia score and Beam Balance score were significantly worse compared to the sham group. The administration of EPZ6438 (3mg/kg) significantly increased both Modified Garcia Score and Beam Balance score at 24h after SAH. The brain water content in the left hemisphere and right hemisphere was significantly increased in the SAH+vehicle group compared to the sham group, while administration of EPZ6438 significantly reduced brain water content in left hemisphere. However, there were no significant differences of the brain water content in the cerebellum and brain stem between sham and SAH groups. (Figure 2A). According to the neurological behavior results, EPZ6438 at 3mg/kg was chosen for the following study.

EPZ6438 administration reduced microglial activation and neutrophil infiltration, and induced the conversion of M1 into M2 at 24h at SAH

To explore the effect of EPZ6438 on neuroinflammation, immunofluorescence staining for microglia activation, neutrophil infiltration, and microglia phenotypes was performed. At 24h after SAH, microglia were activated, as demonstrated by increased Iba-1 positive cells, bigger soma size, and less ramified morphology compared to the quiescent microglia in sham group. EPZ6438 treatment decreased the number of Iba-1 positive cells and reduced the soma size of microglia compared to the vehicle group. (Figure 2B) In addition, MPO-positive cells (considered as neutrophil) were significantly increased in SAH + vehicle group compared with the sham group, while EPZ6438 effectively reduced neutrophil infiltration compared to the vehicle group. (Figure 2C) In addition, EPZ6438 significantly decreased CD16 positive cells (M1 microglia) compared to the vehicle group, while increased CD206 positive cells (M2 microglia). (Figure 2D)

EPZ6438 treatment improved long-term neurobehavioral deficits after SAH.

To assess the sensorimotor coordination of rats, the rotarod test was performed on days 7, 14, and 21. Compared to the sham group, the falling latency was significantly shorter at both 5 rpm and 10 rpm in the SAH + vehicle. EPZ6438 treatment improved the performance of rotarod test compared to the vehicle group. (Figure 3A)

In the water maze test, the escape latency was much longer, and the rats travelled a greater distance to find the platform in the SAH + vehicle group on day 3 and day 4 compared to sham group. EPZ6438 treatment significantly improved the performance on day 3 and day 4 (Figure 3C). In probe quadrant trials, compared to the sham group, the time spent in the target quadrant was significantly decreased in the SAH + vehicle group. EPZ6438 administration notably increased the duration of time that the rats spent in the target quadrant. (Figure 3B)

Inhibition of EZH2 by EPZ6438 attenuated neuroinflammation via H3k27me3/SOCS3/TRAF6/NF-κB pathway after SAH

To explore the underlying anti-neuroinflammatory mechanism of EPZ6438 post SAH, SOCS3 siRNA was injected via *i.c.v* to inhibit the expression of SOCS3. The expression levels of EZH2, H3K27Me3, pathway-related proteins SOCS3, TRAF6, and NF-κB p65, as well as pro-inflammatory cytokines TNF-α, IL-6, and IL-1β were all significantly increased in the SAH + vehicle group compared with the sham group. EPZ6438 treatment significantly decreased the levels of EZH2, H3K27Me3, pathway-related proteins TRAF6, NF-κB p65, and pro-inflammatory cytokines TNF-α, IL-6, IL-1β, but increased the expressions level of SOCS3 and anti-inflammatory cytokine IL-10. However, inhibition of SOCS3 by SOCS3 siRNA abolished the effect of EPZ6438 on SOCS3, TRAF6, NF-κB p65, and pro-inflammatory cytokines TNF-α, IL-6, and IL-1β, as well as anti-inflammatory cytokine IL-10, but had no effect on EZH2 and H3K27Me3. (Figure 4A, B) Consistently, activating H3k27me3 by CRISPR significantly increased the level of H3k27me3 and abolished the effect of EPZ6438. (Figure 5A, B)

Discussion

In the present study, the neuroprotective effect of EPZ6438 and the underlying mechanisms after SAH in rats were explored. The results revealed that at 24h after SAH, the expression levels of EZH2 and H3K27Me3 significantly increased compared to the sham group. EZH2 and H3K27Me3 were co-localized in microglia, neurons, and astrocytes. Inhibition of EZH2 by EPZ6438 improved short- and long- term neurological deficits, ameliorated brain edema, reduced microglial activation, neutrophil infiltration, and induced the conversion of M1 into M2 microglia. EPZ6438 treatment significantly decreased expressions of EZH2 and H3K27Me3 and pro-inflammatory cytokines, but increased expressions of SOCS3 and anti-inflammatory cytokine. Furthermore, SOCS3 siRNA and H3K27Me3 CRISPR abolished the anti-neuroinflammatory effect of EPZ6438, and reversed its effect on the SOCS3/TRAF6/NF-κB signaling pathway. Taken together, our findings indicate that inhibition of EPZ6438, via selective inhibitor EPZ6438, attenuates neuroinflammation after SAH, possibly through the SOCS3/TRAF6/ NF-κB pathway.

There is abundant evidence documenting the relationship between histone methylation and inflammatory diseases.[20–23] Targeting EZH2 methyltransferase activity has been proven to be effective in multiple inflammatory diseases, such as intestinal inflammation, neuropathic pain, and allergic inflammation.[5, 6, 24–26] The inhibition of EZH2 by its inhibitor, GSK343, decreased pro-inflammatory cytokines, delayed onset of colitis, and alleviated the symptoms

of ongoing colitis.[5] Studies have reported that EZH2 deficiency prevented $CD4^+$ T cells and antigen-specific IgE development, and thus inhibited lung inflammation and mucous hypersecretion, the mechanism is possibly due to the requirement of EZH2 in generating antigen-specific memory. Additionally, inhibition of EZH2 by GSK126 significantly ameliorated airway inflammation and hyperresponsiveness in the *in vivo* study.[27, 28] EZH2 played an important role in the immune responses of central nervous system diseases. EZH2 mRNA expression significantly increased in BV-2 microglial cells after the stimulation of lipopolysaccharide. Principal component analysis revealed that genes encoding molecules involved in the response of inflammation were down-regulated after EPZ6438 administration.[7] Similarly, cell-specific knockouts of EZH2, using selective inhibitors, suppressed the activation of microglia after triggering Toll-like receptors.[29] More importantly, EZH2 has been recognized to play a vital role in stroke. The expression of EZH2 was up-regulated in transient middle cerebral artery occlusion model, while inhibition of EZH2 by DZNep suppressed microglial activation, reduced infarct volume, and improved behavioral performance in mice after ischemia.[8] EZH2 promoted neuronal differentiation of human mesenchymal stem cells, and transplantation of human mesenchymal stem cells with EHZ2 knocked out significantly improving the neurological deficits after cerebral ischemia in rats.[30] EZH2, a histone methyltransferase, catalyzes H3K27me3, which in turn controls gene transcription.[31] H3K27me3 demethylase inhibitor, GSK-J4, was proven to suppress microglial activation and exert immunosuppressive effects in macrophages.[32]

SOCS3 is a member of the SOCS family, and is well-known for its role as an intracellular negative regulator of inflammation.[11, 33] SOCS3 gene harbored several EZH2 intervals by ChIP coupled with quantitative PCR assays. Furthermore, compared with the wild type cells, the expression level of SOCS3 was significantly increased in EZH2-deficienct macrophages.[29] As a member of the TNF receptor family, TRAF6 functions in many physiological processes, including cell death and survival.[34, 35] Studies have reported that SOCS3 directly interacted and degraded TRAF6 via hyperubiquitination. A deficiency of TRAF6 paralyzed NF-κB signaling, indicating that TRAF6 also functions as an inflammatory adaptor.[36]

EPZ6438 was the first EZH2 inhibitor to enter clinical trials for its great efficacy in treating non-Hodgkin Lymphoma, and is therefore safe for patients.[37] EPZ6438 inhibits EZH2 in a manner competitive with the substrate S-adenosylmethionine (that is, EPZ6438 and S-adenosylmethionine binding to EZH2 is mutually exclusive, such that only one or the other ligand can bind, but both cannot bind to the enzyme simultaneously), and noncompetitive with the peptide or nucleosome substrate (that is, EPZ6438 binding is not mutually exclusive or synergistic with binding of the peptide/nucleosome substrate of the enzymatic reactions).[10, 38] However, the efficacy of EPZ6438 in inflammatory diseases remains under investigation. As mentioned above, EPZ6438 treatment repressed pro-inflammatory genes in BV-2 microglial cells. Consistently, the present study showed that inhibition of EZH2 by EPZ6438 significantly reduced inflammatory cytokines, improved short- and long-term outcome after SAH in rats, and that the neuroprotective effect of EPZ6438 could be partly reversed by SOCS3 siRNA. Taken together, our results suggested that the SOCS3/TRAF6/NF-κB signaling pathway may underlie the anti-neuroinflammatory and neuroprotective effects of EPZ6438 after SAH.

There are still some limitations in the present study. First, this study mainly focused on neuroinflammation, however, the effects of EZH2 inhibition on other mechanisms, such as apoptosis and blood-brain barrier breakdown, after SAH are required to be investigated. Second, our study and previous study indicated EPZ6438 treatment decreased the expression level of EZH2,[7] but the mechanisms need to be further explored. At last, we demonstrated the important role of SOCS3/TRAF6/NF-κB signaling in the anti-neuroinflammatory effect of EZH2 inhibition. However, other signaling pathways underlying this effect should also be addressed in the future.

Conclusions

We concluded that the inhibition of EZH2 by EPZ6438 reduced neuroinflammation via H3K27Me3/ SOCS3/TRAF6/NF-κB after SAH in rats. EZH2 inhibition may provide a promising therapeutic strategy for SAH.

Supplementary Material

Refer to Web version on PubMed Central for supplementary material.

Sources of Funding

This study was supported by National Natural Science Foundation of China, No. 81971107, and the Fundamental Research Funds for the Central Universities, China, No. 2019QNA7038 to Dr. Sheng Chen, and by the grants from National Institutes of Health(NS081740 and NS082184) to Prof. John H. Zhang.

References

1. Fujii M, Yan J, Rolland WB, Soejima Y, Caner B, Zhang JH. Early brain injury, an evolving frontier in subarachnoid hemorrhage research. Transl Stroke Res. 2013;4:432–446 [PubMed: 23894255]
2. Suzuki H What is early brain injury? Transl Stroke Res. 2015;6:1–3 [PubMed: 25502277]
3. Sehba FA, Hou J, Pluta RM, Zhang JH. The importance of early brain injury after subarachnoid hemorrhage. Prog Neurobiol. 2012;97:14–37 [PubMed: 22414893]
4. Yamagishi M, Uchimaru K. Targeting ezh2 in cancer therapy. Curr Opin Oncol. 2017;29:375–381 [PubMed: 28665819]
5. Zhou J, Huang S, Wang Z, Huang J, Xu L, Tang X, Wan YY, Li QJ, Symonds ALJ, Long H, et al. Targeting ezh2 histone methyltransferase activity alleviates experimental intestinal inflammation. Nat Commun. 2019;10:2427 [PubMed: 31160593]
6. Nakanishi Y, Reina-Campos M, Nakanishi N, Llado V, Elmen L, Peterson S, Campos A, De SK, Leitges M, Ikeuchi H, et al. Control of paneth cell fate, intestinal inflammation, and tumorigenesis by pkclambda/iota. Cell Rep. 2016;16:3297–3310 [PubMed: 27653691]
7. Arifuzzaman S, Das A, Kim SH, Yoon T, Lee YS, Jung KH, Chai YG. Selective inhibition of ezh2 by a small molecule inhibitor regulates microglial gene expression essential for inflammation. Biochem Pharmacol. 2017;137:61–80 [PubMed: 28431938]
8. Chen J, Zhang M, Zhang X, Fan L, Liu P, Yu L, Cao X, Qiu S, Xu Y. Ezh2 inhibitor dznep modulates microglial activation and protects against ischaemic brain injury after experimental stroke. Eur J Pharmacol. 2019;857:172452 [PubMed: 31202798]
9. Brach D, Johnston-Blackwell D, Drew A, Lingaraj T, Motwani V, Warholic NM, Feldman I, Plescia C, Smith JJ, Copeland RA, et al. Ezh2 inhibition by tazemetostat results in altered dependency on b-cell activation signaling in dlbcl. Mol Cancer Ther. 2017;16:2586–2597 [PubMed: 28835384]
10. Knutson SK, Kawano S, Minoshima Y, Warholic NM, Huang KC, Xiao Y, Kadowaki T, Uesugi M, Kuznetsov G, Kumar N, et al. Selective inhibition of ezh2 by epz-6438 leads to potent antitumor

activity in ezh2-mutant non-hodgkin lymphoma. Mol Cancer Ther. 2014;13:842–854 [PubMed: 24563539]

11. Carow B, Rottenberg ME. Socs3, a major regulator of infection and inflammation. Front Immunol. 2014;5:58 [PubMed: 24600449]
12. Williams JJ, Munro KM, Palmer TM. Role of ubiquitylation in controlling suppressor of cytokine signalling 3 (socs3) function and expression. Cells. 2014;3:546–562 [PubMed: 24886706]
13. Guo Z, Hu Q, Xu L, Guo ZN, Ou Y, He Y, Yin C, Sun X, Tang J, Zhang JH. Lipoxin a4 reduces inflammation through formyl peptide receptor 2/p38 mapk signaling pathway in subarachnoid hemorrhage rats. Stroke. 2016;47:490–497 [PubMed: 26732571]
14. Zhou K, Enkhjargal B, Xie Z, Sun C, Wu L, Malaguit J, Chen S, Tang J, Zhang J, Zhang JH. Dihydrolipoic acid inhibits lysosomal rupture and nlrp3 through lysosome-associated membrane protein-1/calcium/calmodulin-dependent protein kinase ii/tak1 pathways after subarachnoid hemorrhage in rat. Stroke. 2018;49:175–183 [PubMed: 29273596]
15. Sugawara T, Ayer R, Jadhav V, Zhang JH. A new grading system evaluating bleeding scale in filament perforation subarachnoid hemorrhage rat model. J Neurosci Methods. 2008;167:327–334 [PubMed: 17870179]
16. Hatashita S, Hoff JT, Salamat SM. Ischemic brain edema and the osmotic gradient between blood and brain. J Cereb Blood Flow Metab. 1988;8:552–559 [PubMed: 3392116]
17. Garcia JH, Wagner S, Liu KF, Hu XJ. Neurological deficit and extent of neuronal necrosis attributable to middle cerebral artery occlusion in rats. Statistical validation. Stroke. 1995;26:627–634; discussion 635 [PubMed: 7709410]
18. Xie Z, Enkhjargal B, Wu L, Zhou K, Sun C, Hu X, Gospodarev V, Tang J, You C, Zhang JH. Exendin-4 attenuates neuronal death via glp-1r/pi3k/akt pathway in early brain injury after subarachnoid hemorrhage in rats. Neuropharmacology. 2018;128:142–151 [PubMed: 28986282]
19. Chen J, Wang L, Wu C, Hu Q, Gu C, Yan F, Li J, Yan W, Chen G. Melatonin-enhanced autophagy protects against neural apoptosis via a mitochondrial pathway in early brain injury following a subarachnoid hemorrhage. J Pineal Res. 2014;56:12–19 [PubMed: 24033352]
20. Alam R, Abdolmaleky HM, Zhou JR. Microbiome, inflammation, epigenetic alterations, and mental diseases. Am J Med Genet B Neuropsychiatr Genet. 2017;174:651–660 [PubMed: 28691768]
21. Horsburgh S, Robson-Ansley P, Adams R, Smith C. Exercise and inflammation-related epigenetic modifications: Focus on DNA methylation. Exerc Immunol Rev. 2015;21:26–41 [PubMed: 25826329]
22. Shen J, Abu-Amer Y, O'Keefe RJ, McAlinden A. Inflammation and epigenetic regulation in osteoarthritis. Connect Tissue Res. 2017;58:49–63 [PubMed: 27389927]
23. Wen KX, Milic J, El-Khodor B, Dhana K, Nano J, Pulido T, Kraja B, Zaciragic A, Bramer WM, Troup J, et al. The role of DNA methylation and histone modifications in neurodegenerative diseases: A systematic review. PLoS One. 2016;11:e0167201 [PubMed: 27973581]
24. Hui T, A P, Zhao Y, Yang J, Ye L, Wang C. Ezh2 regulates dental pulp inflammation by direct effect on inflammatory factors. Arch Oral Biol. 2018;85:16–22 [PubMed: 29028630]
25. Lou X, Zhu H, Ning L, Li C, Li S, Du H, Zhou X, Xu G. Ezh2 regulates intestinal inflammation and necroptosis through the jnk signaling pathway in intestinal epithelial cells. Dig Dis Sci. 2019
26. Yadav R, Weng HR. Ezh2 regulates spinal neuroinflammation in rats with neuropathic pain. Neuroscience. 2017;349:106–117 [PubMed: 28257897]
27. Keenan CR, Iannarella N, Garnham AL, Brown AC, Kim RY, Horvat JC, Hansbro PM, Nutt SL, Allan RS. Polycomb repressive complex 2 is a critical mediator of allergic inflammation. JCI Insight. 2019;4
28. Tumes DJ, Onodera A, Suzuki A, Shinoda K, Endo Y, Iwamura C, Hosokawa H, Koseki H, Tokoyoda K, Suzuki Y, et al. The polycomb protein ezh2 regulates differentiation and plasticity of cd4(+) t helper type 1 and type 2 cells. Immunity. 2013;39:819–832 [PubMed: 24238339]
29. Zhang X, Wang Y, Yuan J, Li N, Pei S, Xu J, Luo X, Mao C, Liu J, Yu T, et al. Macrophage/microglial ezh2 facilitates autoimmune inflammation through inhibition of socs3. J Exp Med. 2018;215:1365–1382 [PubMed: 29626115]

30. Yu YL, Chou RH, Shyu WC, Hsieh SC, Wu CS, Chiang SY, Chang WJ, Chen JN, Tseng YJ, Lin YH, et al. Smurf2-mediated degradation of ezh2 enhances neuron differentiation and improves functional recovery after ischaemic stroke. EMBO Mol Med. 2013;5:531–547 [PubMed: 23526793]

31. Luo H, Jiang Y, Ma S, Chang H, Yi C, Cao H, Gao Y, Guo H, Hou J, Yan J, et al. Ezh2 promotes invasion and metastasis of laryngeal squamous cells carcinoma via epithelial-mesenchymal transition through h3k27me3. Biochem Biophys Res Commun. 2016;479:253–259 [PubMed: 27638307]

32. Das A, Arifuzzaman S, Yoon T, Kim SH, Chai JC, Lee YS, Jung KH, Chai YG. Rna sequencing reveals resistance of tlr4 ligand-activated microglial cells to inflammation mediated by the selective jumonji h3k27 demethylase inhibitor. Sci Rep. 2017;7:6554 [PubMed: 28747667]

33. Qin H, Holdbrooks AT, Liu Y, Reynolds SL, Yanagisawa LL, Benveniste EN. Socs3 deficiency promotes m1 macrophage polarization and inflammation. J Immunol. 2012;189:3439–3448 [PubMed: 22925925]

34. Luo Z, Zhang X, Zeng W, Su J, Yang K, Lu L, Lim CB, Tang W, Wu L, Zhao S, et al. Traf6 regulates melanoma invasion and metastasis through ubiquitination of basigin. Oncotarget. 2016;7:7179–7192 [PubMed: 26769849]

35. Schimmack G, Schorpp K, Kutzner K, Gehring T, Brenke JK, Hadian K, Krappmann D. Yod1/traf6 association balances p62-dependent il-1 signaling to nf-kappab. Elife. 2017;6

36. Zhou X, Liu Z, Cheng X, Zheng Y, Zeng F, He Y. Socs1 and socs3 degrades traf6 via polyubiquitination in lps-induced acute necrotizing pancreatitis. Cell Death Dis. 2015;6:e2012 [PubMed: 26633718]

37. Gulati N, Beguelin W, Giulino-Roth L. Enhancer of zeste homolog 2 (ezh2) inhibitors. Leuk Lymphoma. 2018;59:1574–1585 [PubMed: 29473431]

38. McCabe MT, Ott HM, Ganji G, Korenchuk S, Thompson C, Van Aller GS, Liu Y, Graves AP, Della Pietra A 3rd, Diaz E, et al. Ezh2 inhibition as a therapeutic strategy for lymphoma with ezh2-activating mutations. Nature. 2012;492:108–112 [PubMed: 23051747]

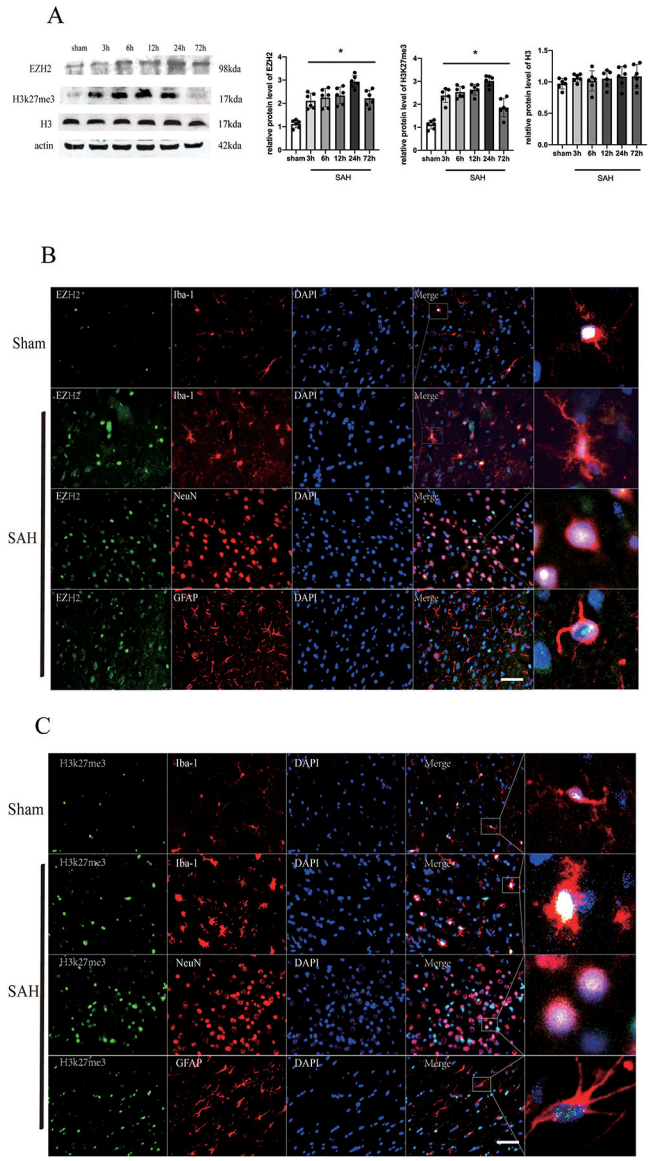

Figure 1. Expression of EZH2 and H3K27me3 after SAH

(A) Representative Western blot images and quantitative analyses of EZH2 and H3K27me3 time course after SAH. n=6 per group. (B) Double immunofluorescence staining for EZH2 (green) in the neuron (NeuN, red), astrocytes (GFAP, red) and microglia (Iba-1, red) in the left basal cortex at 24h after SAH. n=2 per group. (C) Double immunofluorescence staining for H3K27Me3 (green) in the neuron (NeuN, red), astrocytes (GFAP, red) and microglia (Iba-1, red) in the left basal cortex at 24h after SAH. n=2 per group. One-way ANOVA. *P<0.05 vs. sham group. Bars represent mean ± SD. Scale bar = 50 μm.

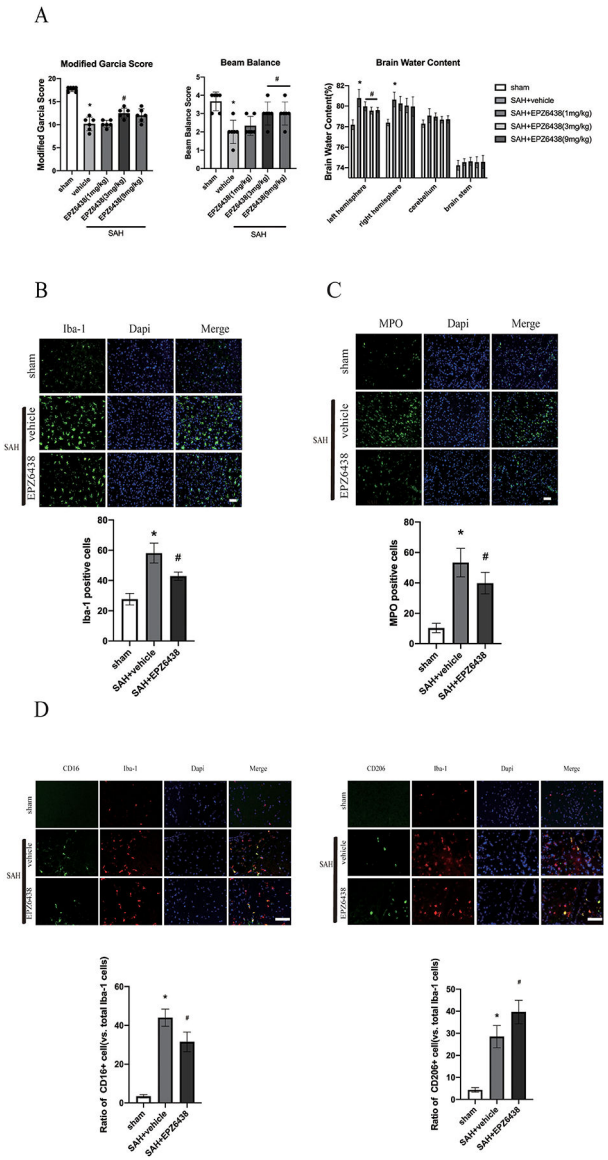

Figure 2. EPZ6438 improved the short-term neurobehavior after SAH

(A) Modified Garcia score, beam balance score and brain water content. n=6 per group. (B) Immunofluorescence staining for microglia (Iba-1). n=3 per group. Scale bar = 20 μm. (C) Immunofluorescence staining for neutrophil (MPO). n=3 per group. Scale bar = 20 μm. (D) Immunofluorescence staining for M1 (CD16) and M2 (CD206) microglia. n=3 per group. Scale bar = 40 μm. One-way and two-way (brain water content) ANOVA. *P<0.05 vs. sham group. #P<0.05 vs. SAH + vehicle group. Bars represent mean ± SD.

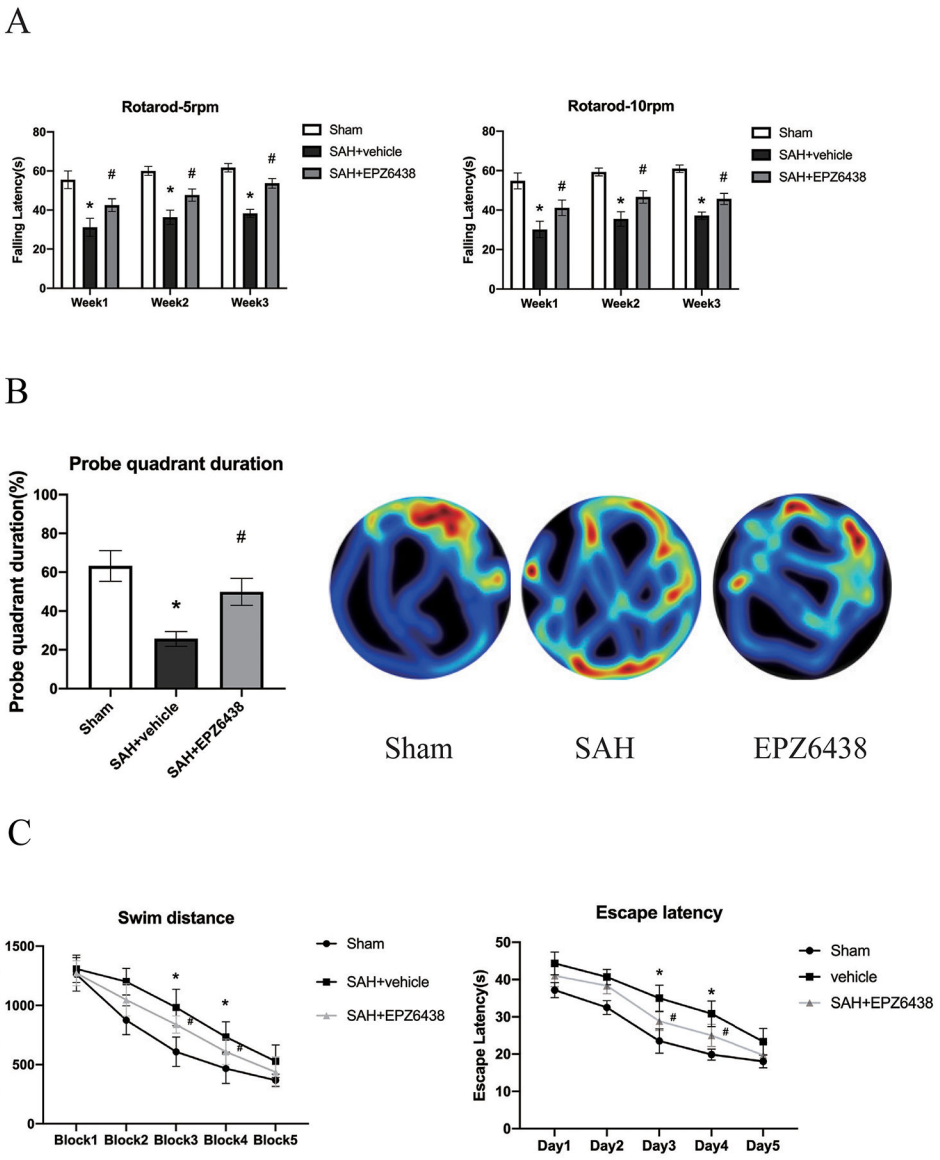

Figure 3. EPZ6438 improved the long-term neurobehavior after SAH

(A) Rotarod test of 5RPM and 10RPM. (B) Probe quadrant duration and typical traces of water maze. (C) Swim distance and escape latency. n=10 per group. One-way (B) and Two-way (A, C) ANOVA. *P<0.05 vs. sham group. #P<0.05 vs. SAH + vehicle group. Bars represent mean ± SD.

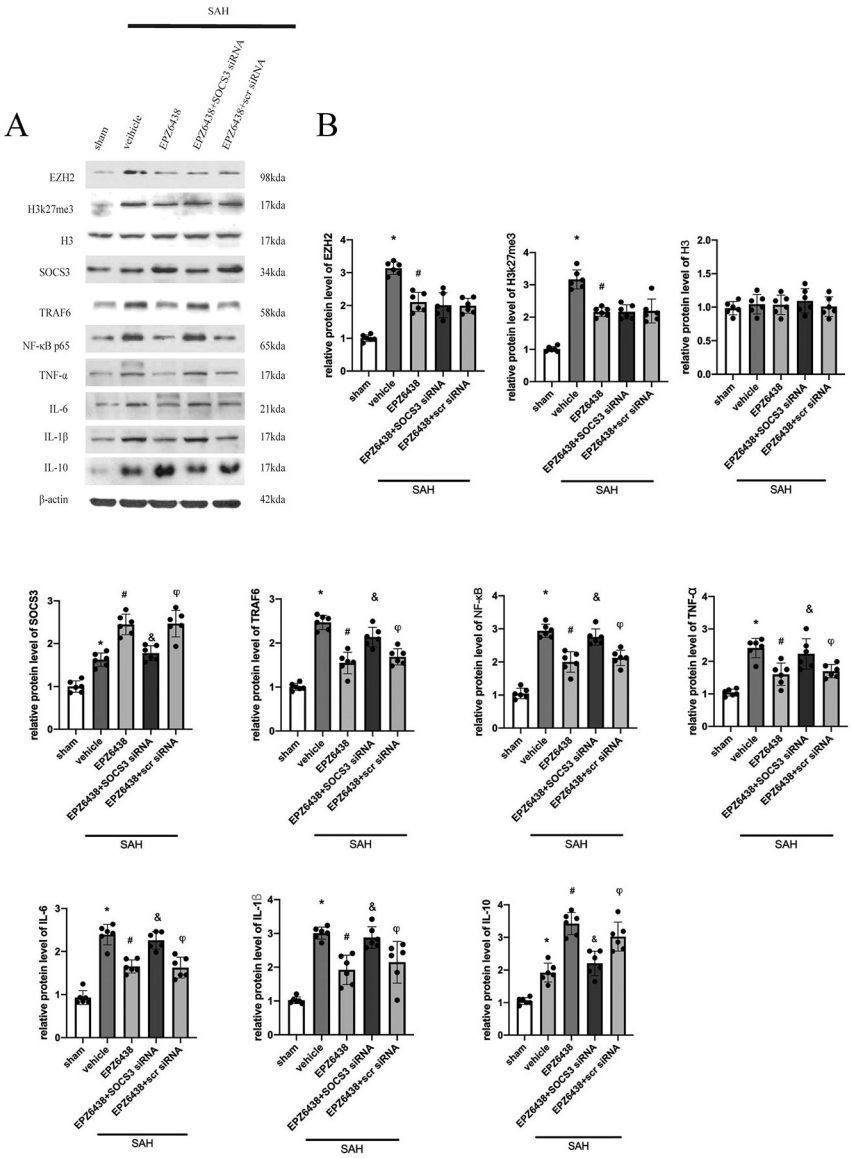

Figure 4. The effects of SOCS3 siRNA in the protein expression of EZH2, H3K27me3, H3, SOCS3, TRAF6, NF-κB, TNF-α, IL-6, IL-1β, IL-10.

(A)Representative Western blot images and quantitative analyses (B) of EZH2, H3K27me3, H3, SOCS3, TRAF6, NF-κB, TNF-α, IL-6, IL-1β, IL-10. One-way ANOVA. *P<0.05 vs. sham group. #P<0.05 vs. SAH + vehicle group. &P<0.05 vs. SAH + EPZ6438 group. φP<0.05 vs. SAH+EPZ6438+SOCS3 siRNA group. Bars represent mean ± SD.

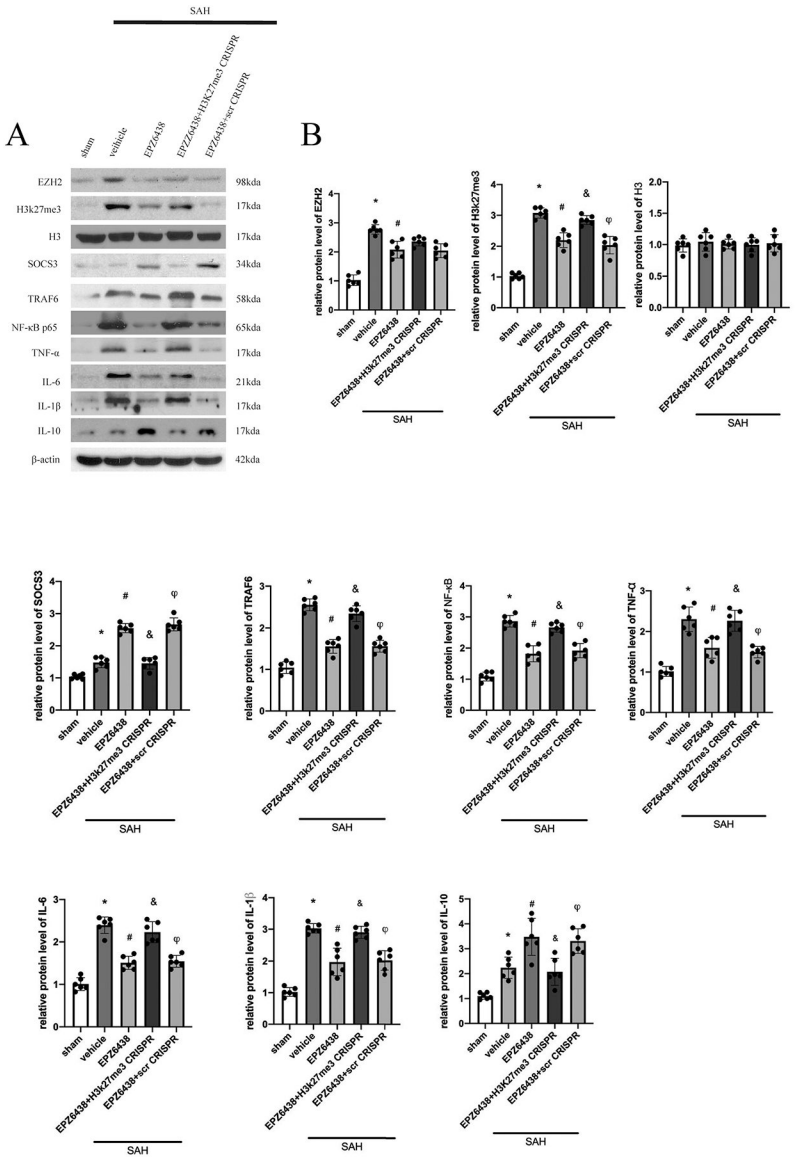

Figure 5. The effects of H3K27me3 CRISPR in the protein expression of EZH2, H3K27me3, H3, SOCS3, TRAF6, NF-κB, TNF-α, IL-6, IL-1β, IL-10.

(A)Representative Western blot images and quantitative analyses (B) of EZH2, H3K27me3, H3, SOCS3, TRAF6, NF-κB, TNF-α, IL-6, IL-1β, IL-10. *P<0.05 vs. sham group. #P<0.05 vs. SAH + vehicle group. &P<0.05 vs. SAH + EPZ6438 group. φP<0.05 vs. SAH +EPZ6438+H3K27me3 CRISPR group. Bars represent mean ± SD.